The Transition Between "Soft" & "Hard" Scattering

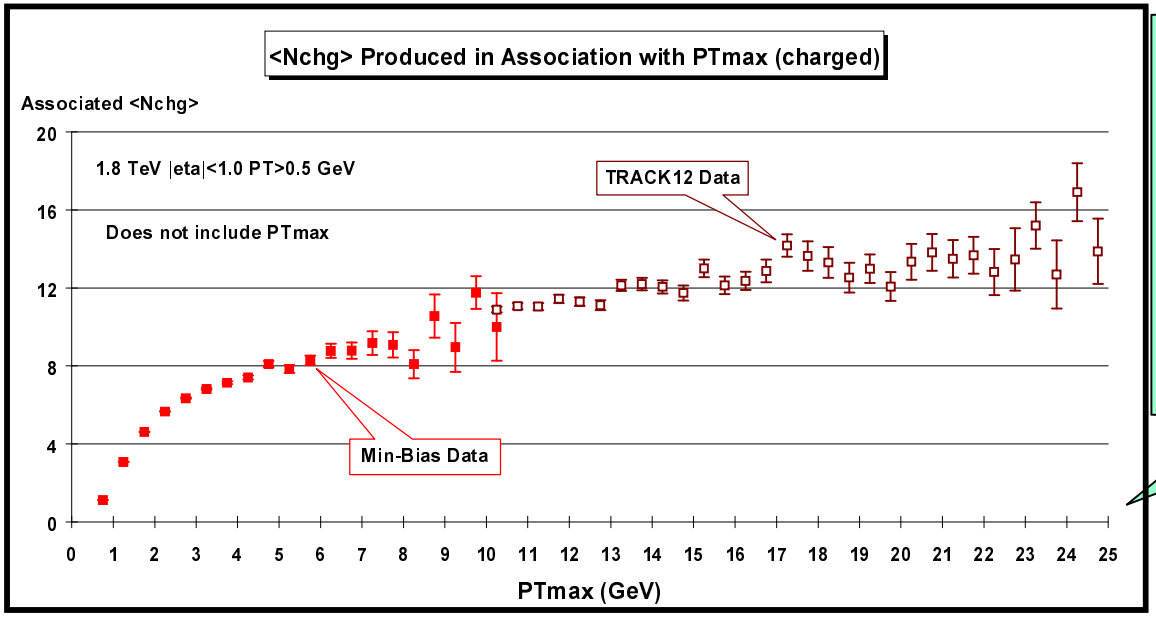

Fig. 3.1. Average number of "associated" charged particles ($P_T > 0.5$ GeV and $|\eta| < 1$) as a function of PTmax (*leading charged particle*). Each point corresponds to the <Nchg> in a 0.5 GeV bin (*not including PTmax*). The solid (open) points are the Min-Bias data (TRACK12 data). The data have not been corrected for efficiency.

Field-Stuart CDF#5067

- **Plot shows "associated" <Nchg> versus PTmax. Each point corresponds to the <Nchg> in a 0.5 GeV bin (*not including PTmax*).**
- **Only consider charged particles with $|\eta| < 1$ and $P_T > 0.5$ GeV where the efficiency is good and use TRACK12 data to extend to large PTmax (highest PT charged particle in the event).**

The Transition Between "Soft" & "Hard" Scattering

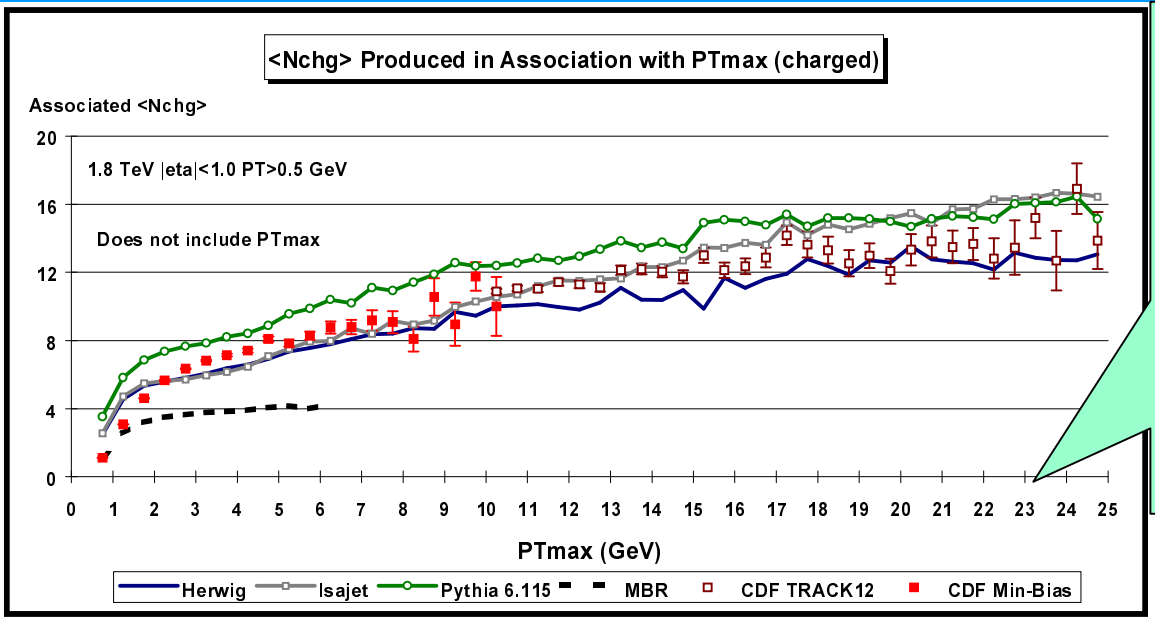

Fig. 3.2. Data on the average number of "associated" charged particles ($P_T > 0.5$ GeV and $|\eta| < 1$) as a function of PTmax (*leading charged particle*) from Fig. 3.1 compared with the QCD "hard" scattering Monte-Carlo predictions of Herwig 5.9, Isajet 7.32, Pythia 6.115, and the "soft" scattering predictions of MBR. Each point corresponds to the <Nchg> in a 0.5 GeV bin (*not including PTmax*). The theoretical predictions have been corrected for the CTC efficiency.

Field-Stuart CDF#5067

- **Plot shows "associated" <Nchg> versus PTmax. Each point corresponds to the <Nchg> in a 0.5 GeV bin (*not including PTmax*).**
- **Only consider charged particles with $|\eta| < 1$ and $P_T > 0.5$ GeV where the efficiency is good and use TRACK12 data to extend to large PTmax (highest PT charged particle in the event).**
- **Theoretical Monte-Carlo predictions must satisfy the CDF "min-bias" trigger and have been corrected for efficiency.**

Distribution of Nchg Relative to PTmax

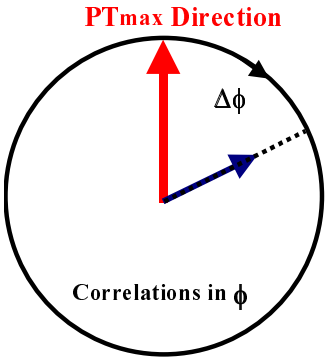

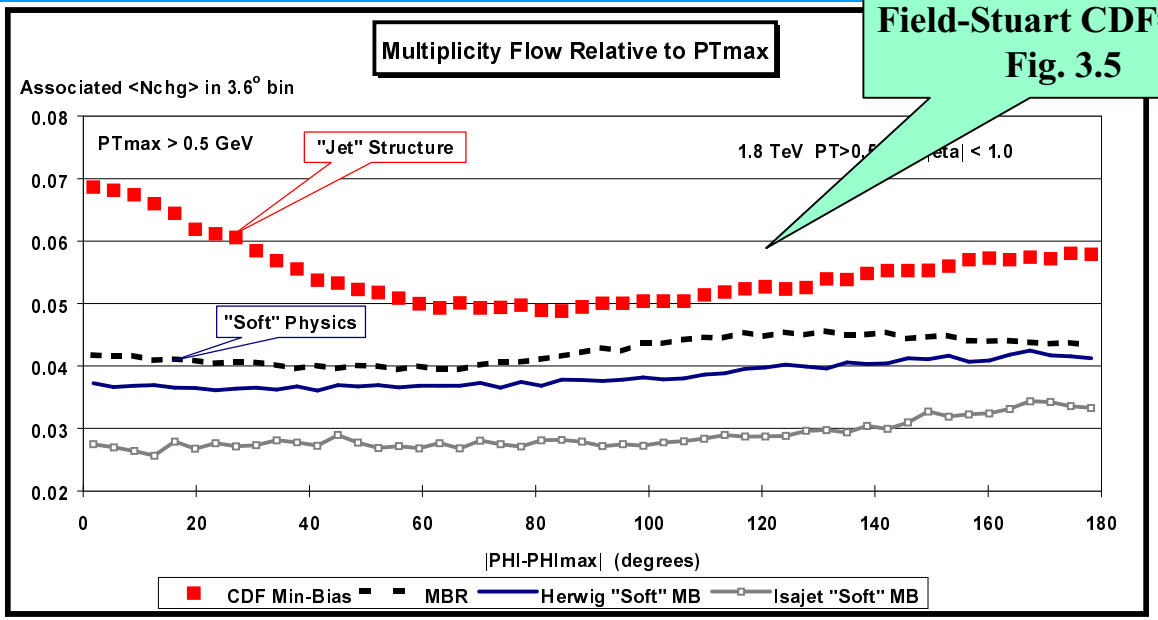

Field-Stuart CDF#5067
Fig. 3.5

<PTmax> = 1.2 GeV

- **Define PTmax to be the highest PT charged particle in the event ($|\eta| < 1$ $P_T > 0.5$ GeV) and look at correlations in ϕ.**
- **Plot shows the associated charged particle multiplicity flow in ϕ relative to PTmax as a function of $|\phi - \phi max|$. Each point corresponds to the <Nchg> in a 3.6^o bin (*not including PTmax*).**
- **"Soft" scattering models have no correlations (except resonances and momentum conservation).**

The Evolution of "Jets" from 0.5 to 50 GeV

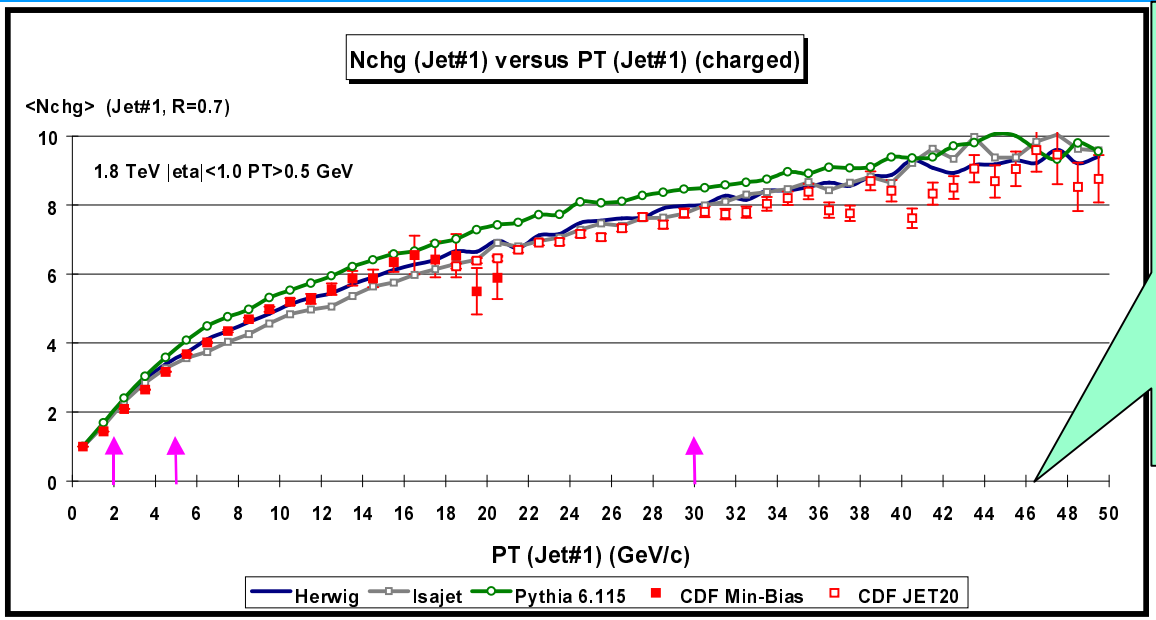

Fig. 4.16. Average number of charged particles in jet#1 *(leading jet)* for charged particles with $P_T > 0.5$ GeV and $|\eta| < 1$ as a function of P_T(jet#1). The solid (open) points are the Min-Bias data (JET20 data). The data are compared with the QCD "hard" scattering Monte-Carlo predictions of Herwig 5.9, Isajet 7.32, and Pythia 6.115 (*corrected for the CTC efficiency*). Jets are defined as "circular regions" (R = 0.7) in η-ϕ space.

Field-Stuart CDF#5067

- **Compares data on the average number of charged particles within Jet#1 (leading jet, R = 0.7) with the QCD "hard" scattering predictions of Herwig 5.9, Isajet 7.32, and Pythia 6.115.**
- **Use the JET20 data to extend the range to 0.5 < PT(jet#1) < 50 GeV. Plot shows <Nchg(jet#1)> versus PT(jet#1).**
- **Only charged particles with $|\eta| < 1$ and $P_T > 0.5$ GeV are included and the theory has been corrected for efficiency.**

Multiplicity Distribution of Nchg within Jet#1

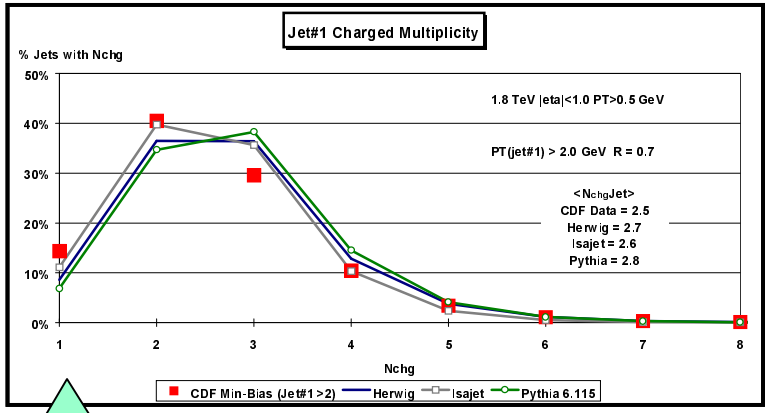

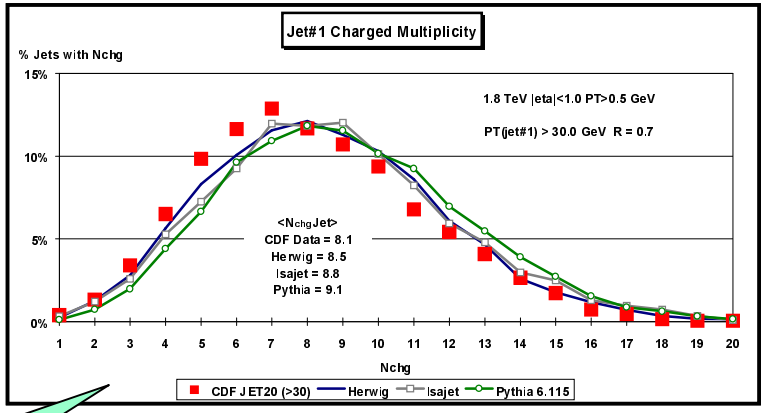

Fig. 4.17
PT(jet#1) > 2 GeV

Fig. 4.19
PT(jet#1) > 30 GeV

Field-Stuart CDF#5067

- **Compares data on the multiplicity distribution of charged particles within Jet#1 (leading jet, R = 0.7) with the QCD "hard" scattering predictions of Herwig 5.9, Isajet 7.32, and Pythia 6.115.**
- **Use the JET20 data to extend the range to 0.5 < PT(jet#1) < 50 GeV. Plot shows the percentage of events in which jet#1 has Nchg charged particles.**
- **Only charged particles with $|\eta| < 1$ and $P_T > 0.5$ GeV are included and the theory has been corrected for efficiency.**

Jet#1 "Size" vs PT(jet#1)

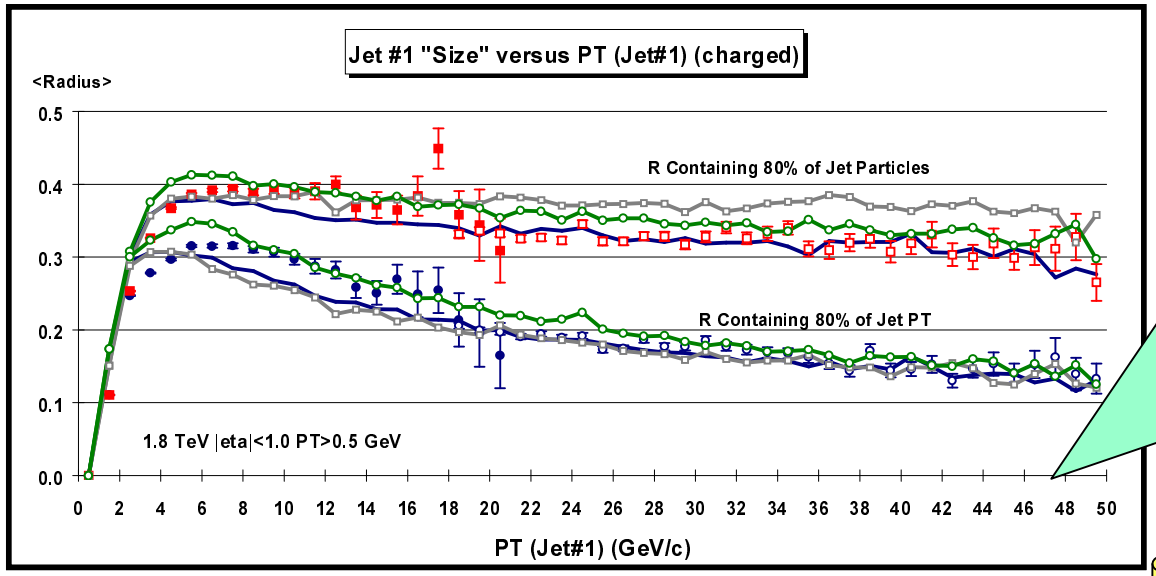

Fig. 4.20-4.22. Average "size" of jet#1 *(leading jet)* for charged particles with $P_T > 0.5$ GeV and $|\eta| < 1$ as a function of P_T(jet#1). The solid (open) points are the Min-Bias data (JET20 data). The squares (circles) correspond the radius in η-ϕ space, R, that contains 80% of the charged particles (80% of the P_T) in jet#1. The data are compared with the QCD "hard" scattering Monte-Carlo predictions of Herwig 5.9. Isajet 7.32, and Pythia 6.115 (*corrected for the CTC efficiency*).

Field-Stuart CDF#5067

- **Compares data on the average radius containing 80% of the particles and 80% of the PT of Jet#1 (leading jet) with the QCD "hard" scattering predictions.**
- **Use the JET20 data to extend the range to 0.5 < PT(jet#1) < 50 GeV. Plot shows <R(jet#1)> versus PT(jet#1).**
- **Only charged particles with $|\eta| < 1$ and $P_T > 0.5$ GeV are included and the theory has been corrected for efficiency.**

Radial Distribution of Nchg within Jet#1

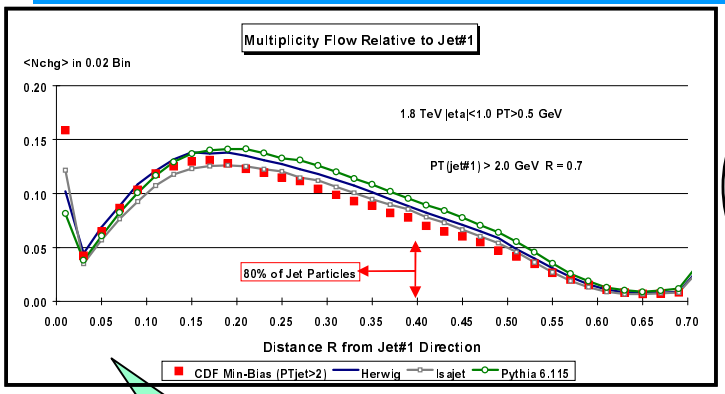

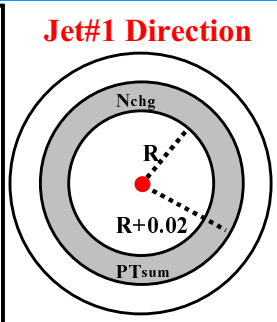

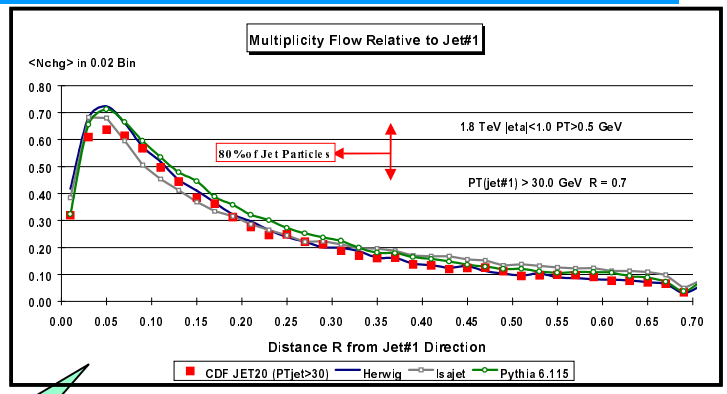

Fig. 4.24
PT(jet#1) > 2 GeV

Fig. 4.28
PT(jet#1) > 30 GeV

Field-Stuart CDF#5067

- **Compares data on the radial distribution of charged particles within Jet#1 (leading jet, R = 0.7) with the QCD "hard" scattering predictions of Herwig 5.9, Isajet 7.32, and Pythia 6.115.**
- **Use the JET20 data to extend the range to 0.5 < PT(jet#1) < 50 GeV. Plot shows the <Nchg> in a 0.02 bin of R, where R is the η–ϕ distance from jet#1.**
- **Only charged particles with $|\eta| < 1$ and $P_T > 0.5$ GeV are included and the theory has been corrected for efficiency.**

Radial Distribution of PTsum within Jet#1

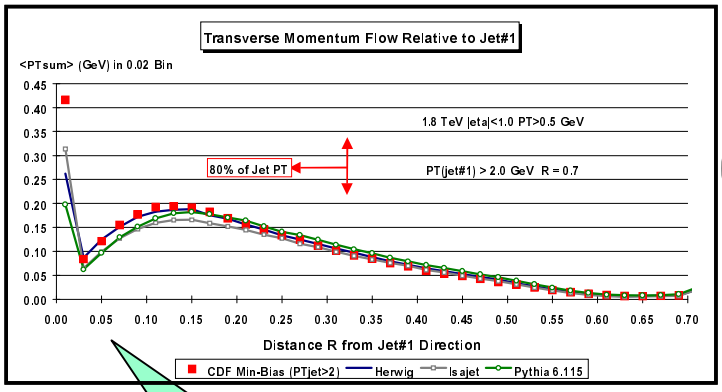

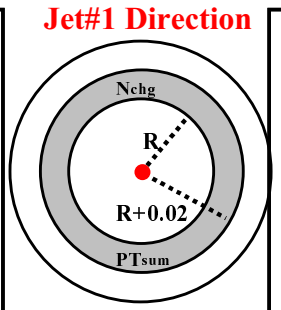

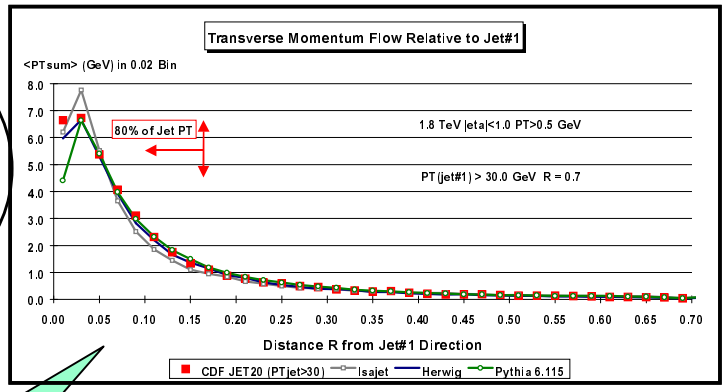

Fig. 4.25
PT(jet#1) > 2 GeV

Fig. 4.29
PT(jet#1) > 30 GeV

Field-Stuart CDF#5067

- **Compares data on the radial distribution of PTsum within Jet#1 (leading jet, R = 0.7) with the QCD "hard" scattering predictions of Herwig 5.9, Isajet 7.32, and Pythia 6.115.**
- **Use the JET20 data to extend the range to 0.5 < PT(jet#1) < 50 GeV. Plot shows the <PTsum> in a 0.02 bin of R, where R is the η–ϕ distance from jet#1.**
- **Only charged particles with $|\eta| < 1$ and $P_T > 0.5$ GeV are included and the theory has been corrected for efficiency.**

Z-Distribution of Charged Particles within Jet#1

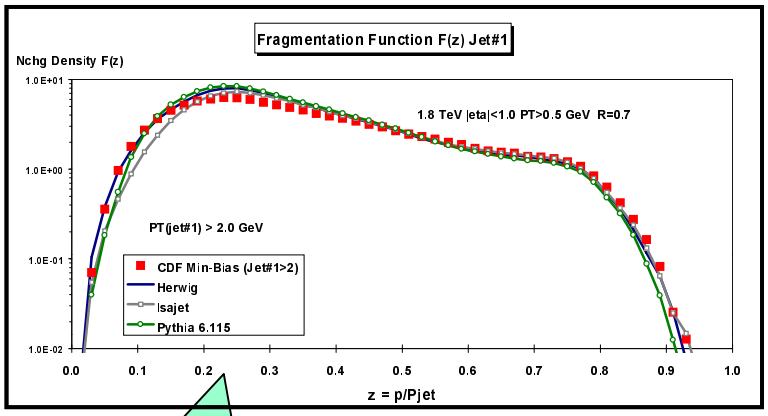

Fig. 4.31
PT(jet#1) > 2 GeV

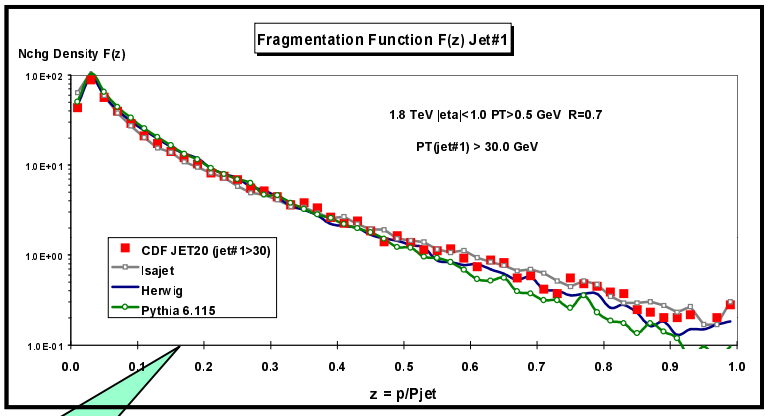

Fig. 4.33
PT(jet#1) > 30 GeV

Field-Stuart CDF#5067

- Compares data on the momentum distribution within Jet#1 (leading jet, R = 0.7) with the QCD "hard" scattering predictions of Herwig 5.9, Isajet 7.32, and Pythia 6.115.
- Use the JET20 data to extend the range to 0.5 < PT(jet#1) < 50 GeV. Plot shows the "charged fragmentation function" F(z) = dNchg/dz, where z = p/P(jet#1).
- Only charged particles with $|\eta| < 1$ and $P_T > 0.5$ GeV are included and the theory has been corrected for efficiency.

Charged Multiplicity versus PT(jet#1)

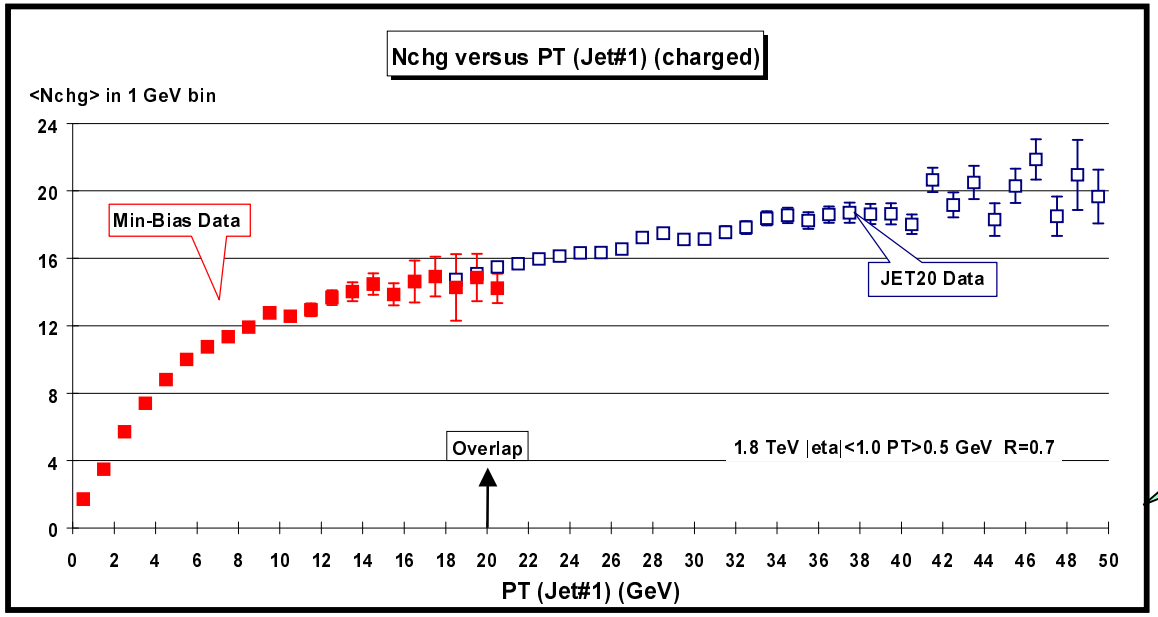

Fig. 4.2. Average number of charged particles ($P_T > 0.5$ GeV and $|\eta| < 1$) as a function of P_T(jet#1) (*leading jet*). Each point corresponds to <Nchg> in a 1 GeV bin. The solid (open) points are the Min-Bias data (JET20 data). The data have not been corrected for efficiency

Field-Stuart CDF#5067

- **Plot shows <Nchg> versus PT(jet#1). Each point corresponds to the <Nchg> in a 1 GeV bin (*including jet#1*).**
- **Only consider charged particles with $|\eta| < 1$ and $P_T > 0.5$ GeV where the efficiency is good and use the JET20 data to extend the range to $0.5 <$ PT(jet#1) < 50 GeV.**

Distribution of Nchg Relative to Jet#1

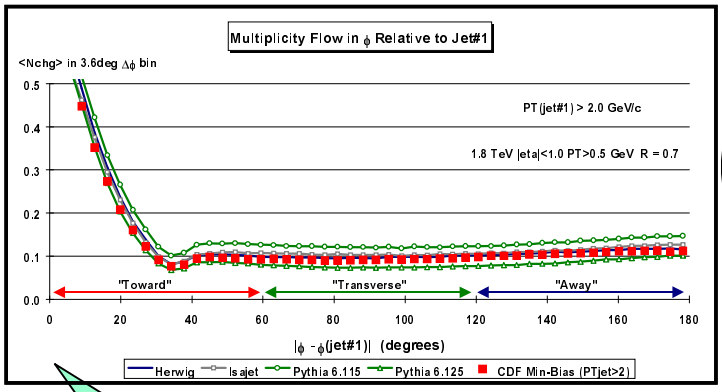

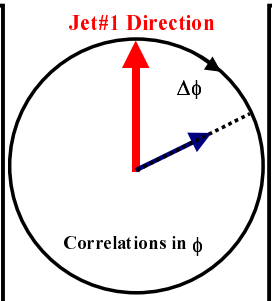

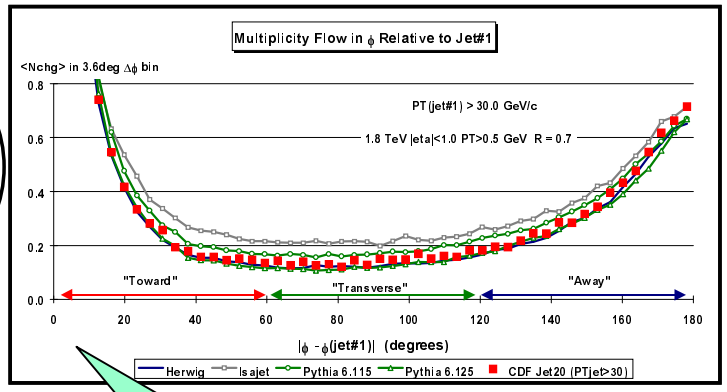

Fig. 5.2
PT(jet#1) > 2 GeV

Field-Stuart CDF#5067

Fig. 5.6
PT(jet#1) > 30 GeV

- Look at the charged multiplicity flow in ϕ relative to the direction of jet#1 ($|\eta| < 1$ $P_T > 0.5$ GeV). Use the JET20 data to extend the range to $0.5 < PT(jet\#1) < 50$ GeV.
- Define "Toward" $|\phi-\phi jet| < 60^o$ (includes jet#1), "Transverse" $60^o < |\phi-\phi jet| < 120^o$, and "Away" $|\phi-\phi jet| < 120^o$ region.
- Plot shows <Nchg> in a 3.6^o $\Delta\phi$ bin compared with the QCD "hard" scattering predictions of Herwig 5.9, Isajet 7.32, Pythia 6.115, and Pythia 6.125.

Distribution of Nchg Relative to Jet#1

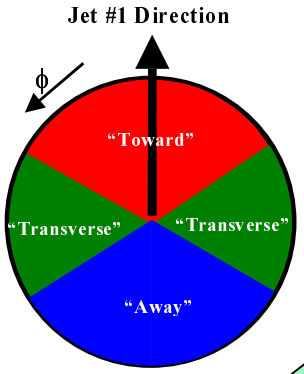

Field-Stuart CDF#5067
Fig. 5.9

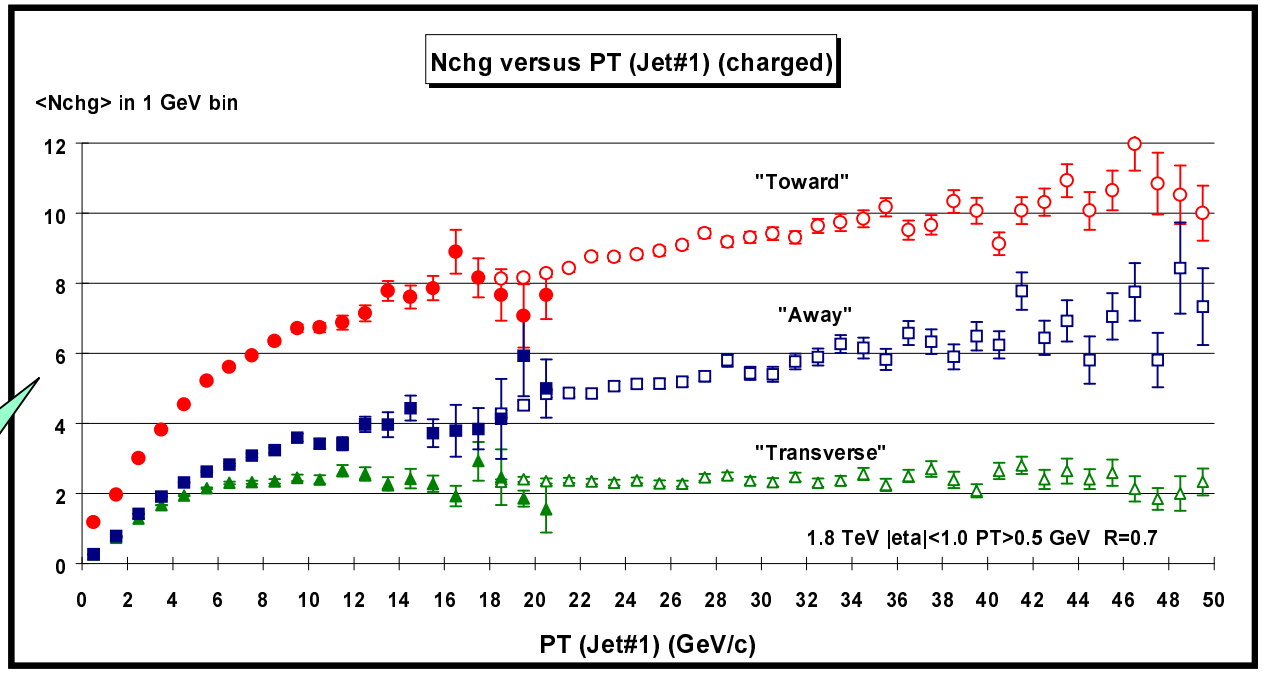

- Look at the charged multiplicity flow in ϕ relative to the direction of jet#1 ($|\eta| < 1$ $P_T > 0.5$ GeV). Use the JET20 data to extend the range to $0.5 <$ PT(jet#1) < 50 GeV.
- Define "Toward" $|\phi - \phi_{jet}| < 60^o$ (includes jet#1), "Transverse" $60^o < |\phi - \phi_{jet}| < 120^o$, and "Away" $|\phi - \phi_{jet}| < 120^o$ region.
- Plot shows <Nchg> in the three regions versus PT(jet#1).

Distribution of PTsum Relative to Jet#1

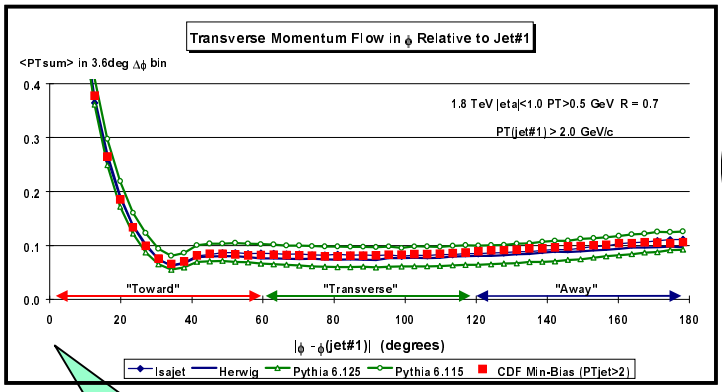

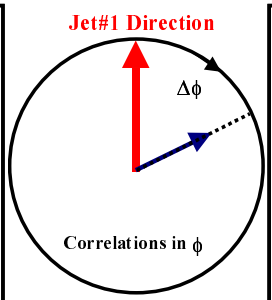

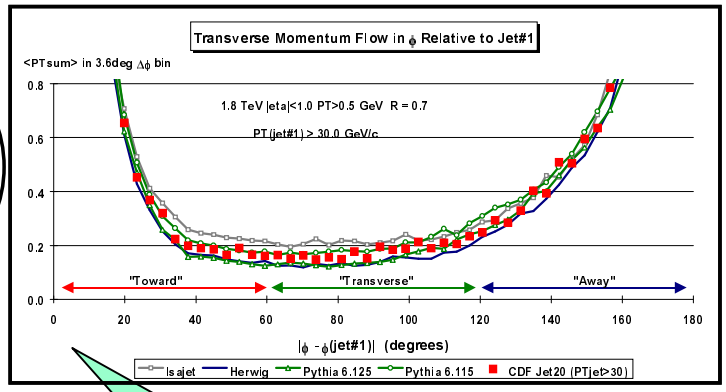

Fig. 5.3
PT(jet#1) > 2 GeV

Field-Stuart CDF#5067

Fig. 5.7
PT(jet#1) > 30 GeV

- Look at the charged PT flow in ϕ relative to the direction of jet#1 ($|\eta| < 1$ $P_T > 0.5$ GeV). Use the JET20 data to extend the range to 0.5 < PT(jet#1) < 50 GeV.
- Define "Toward" $|\phi-\phi jet| < 60^o$ (includes jet#1), "Transverse" $60^o < |\phi-\phi jet| < 120^o$, and "Away" $|\phi-\phi jet| < 120^o$ region.
- Plot shows <PTsum> in a 3.6^o $\Delta\phi$ bin compared with the QCD "hard" scattering predictions of Herwig 5.9, Isajet 7.32, Pythia 6.115, and Pythia 6.125.

Distribution of PTsum Relative to Jet#1

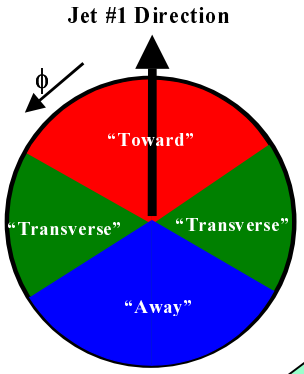

Field-Stuart CDF#5067
Fig. 5.11

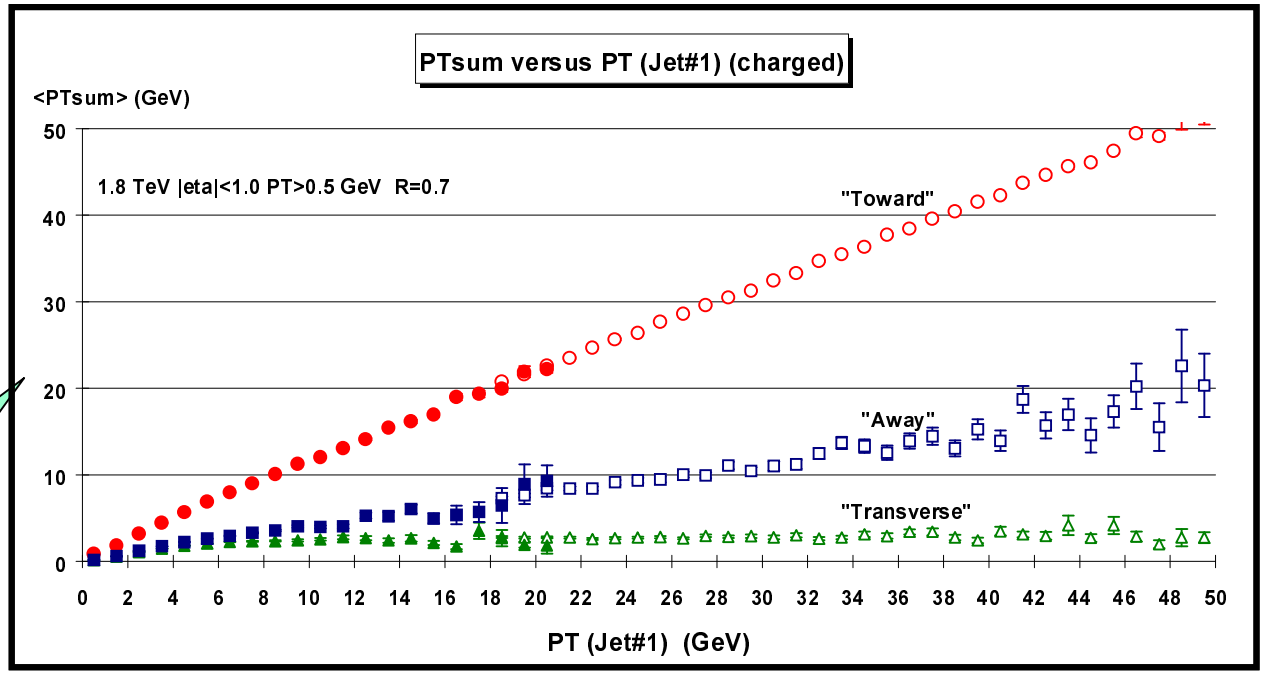

- Look at the PT flow in ϕ relative to the direction of jet#1 ($|\eta| < 1$ $P_T > 0.5$ GeV). Use the JET20 data to extend the range to $0.5 <$ PT(jet#1) < 50 GeV.
- Define "Toward" $|\phi - \phi_{jet}| < 60^o$ (includes jet#1), "Transverse" $60^o < |\phi - \phi_{jet}| < 120^o$, and "Away" $|\phi - \phi_{jet}| < 120^o$ region.
- Plot shows <PTsum> in the three regions versus PT(jet#1).

Distribution of Nchg Relative to Jet#1

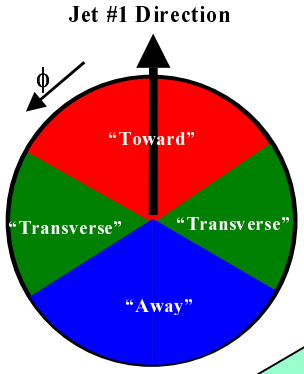

Field-Stuart CDF#5067
Fig. 5.13, 5.15, 5.17

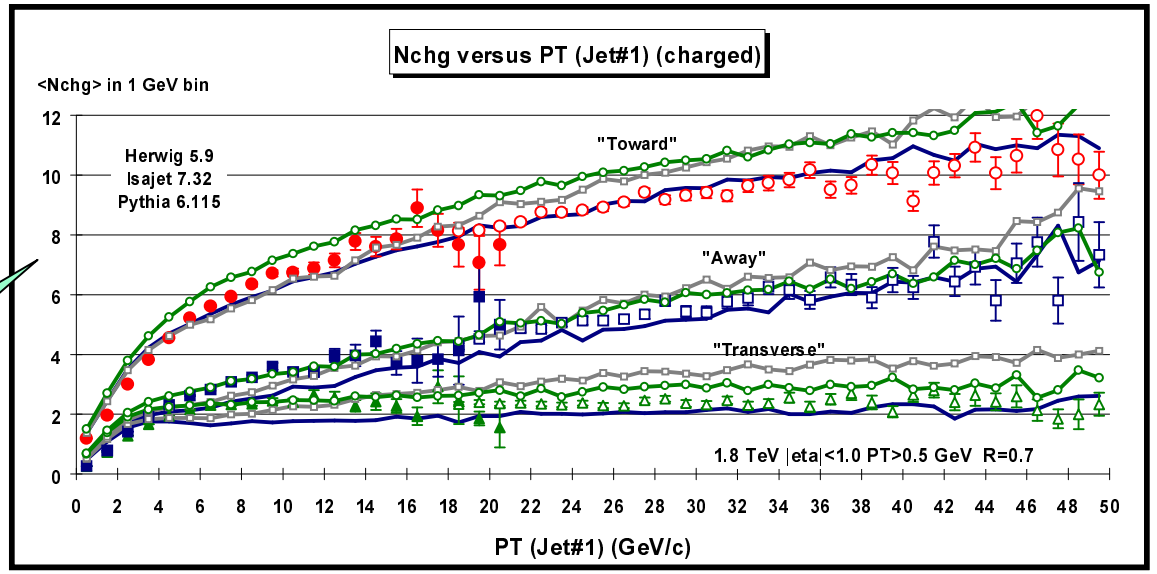

- Look at the charged multiplicity flow in ϕ relative to the direction of jet#1 ($|\eta| < 1$ $P_T > 0.5$ GeV). Use the JET20 data to extend the range to $0.5 < PT(jet\#1) < 50$ GeV.
- Define "Toward" $|\phi-\phi jet| < 60^o$ (includes jet#1), "Transverse" $60^o < |\phi-\phi jet| < 120^o$, and "Away" $|\phi-\phi jet| < 120^o$ region.
- Plot shows <Nchg> in the three regions versus PT(jet#1) compared with the QCD "hard" scattering predictions of Herwig 5.9, Isajet 7.32, and Pythia 6.115.

"Transverse" Nchg versus PT(jet#1)

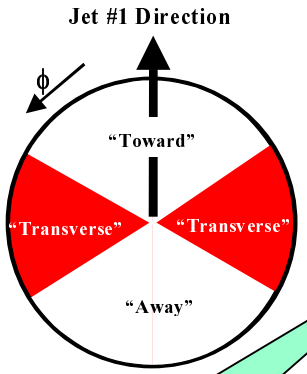

Field-Stuart CDF#5067
Fig. 5.22

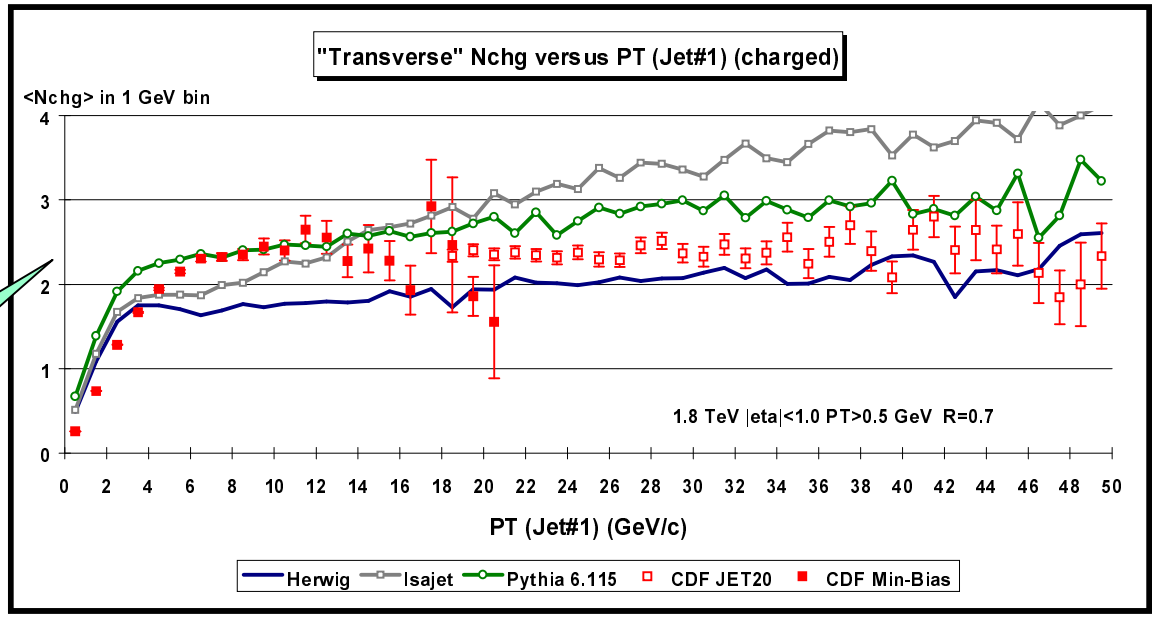

- Look at the charged multiplicity flow in ϕ relative to the direction of jet#1 ($|\eta| < 1$ $P_T > 0.5$ GeV). Use the JET20 data to extend the range to $0.5 <$ PT(jet#1) < 50 GeV. Define "Transverse" $60^o < |\phi - \phi jet| < 120^o$.
- Plot shows "Transverse" <Nchg> in the vs PT(jet#1) compared to the QCD "hard" scattering predictions of Herwig 5.9, Isajet 7.32, and Pythia 6.115.

"Transverse" PTsum versus PT(jet#1)

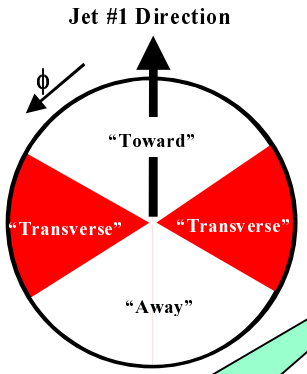

Field-Stuart CDF#5067
Fig. 5.23

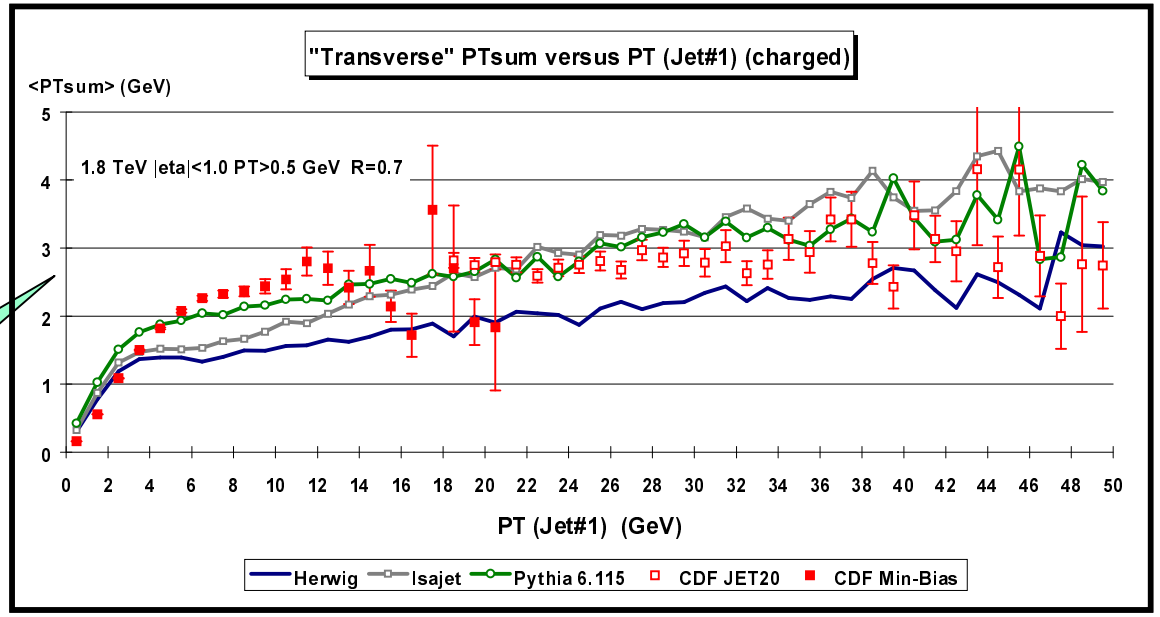

- Look at the charged PT flow in ϕ relative to the direction of jet#1 ($|\eta| < 1$ $P_T > 0.5$ GeV). Use the JET20 data to extend the range to 0.5 < PT(jet#1) < 50 GeV. Define "Transverse" $60^o < |\phi - \phi jet| < 120^o$.
- Plot shows "Transverse" <PTsum> in the vs PT(jet#1) compared to the QCD "hard" scattering predictions of Herwig 5.9, Isajet 7.32, and Pythia 6.115.

"Transverse" Nchg versus PT(jet#1)

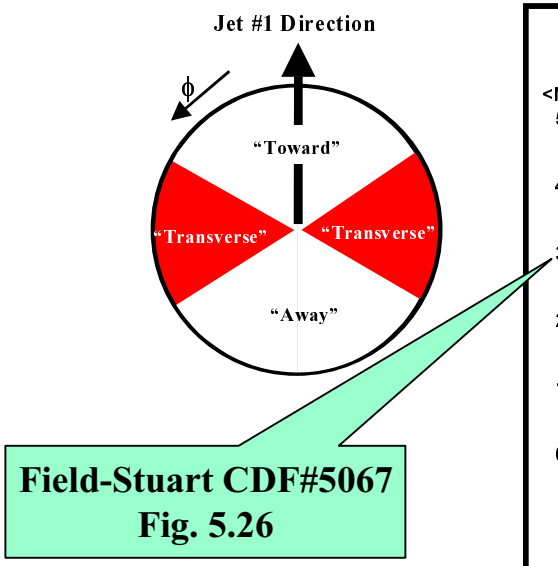

Field-Stuart CDF#5067
Fig. 5.26

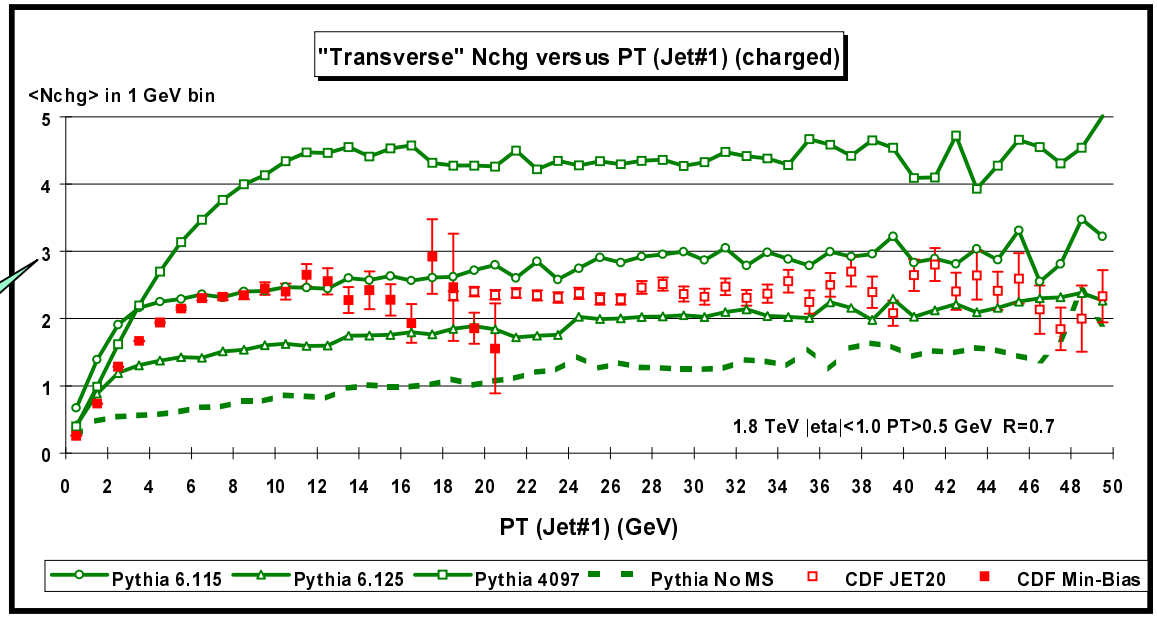

- Look at the charged multiplicity flow in ϕ relative to the direction of jet#1 ($|\eta| < 1$ $P_T > 0.5$ GeV). Use the JET20 data to extend the range to $0.5 <$ PT(jet#1) < 50 GeV. Define "Transverse" $60^o < |\phi - \phi jet| < 120^o$.
- Plot shows "Transverse" <Nchg> in the vs PT(jet#1) compared to the QCD "hard" scattering predictions of four versions of Pythia (6.115, 6.125, no multiple interactions, and CDF note 4097).

"Transverse" PTsum versus PT(jet#1)

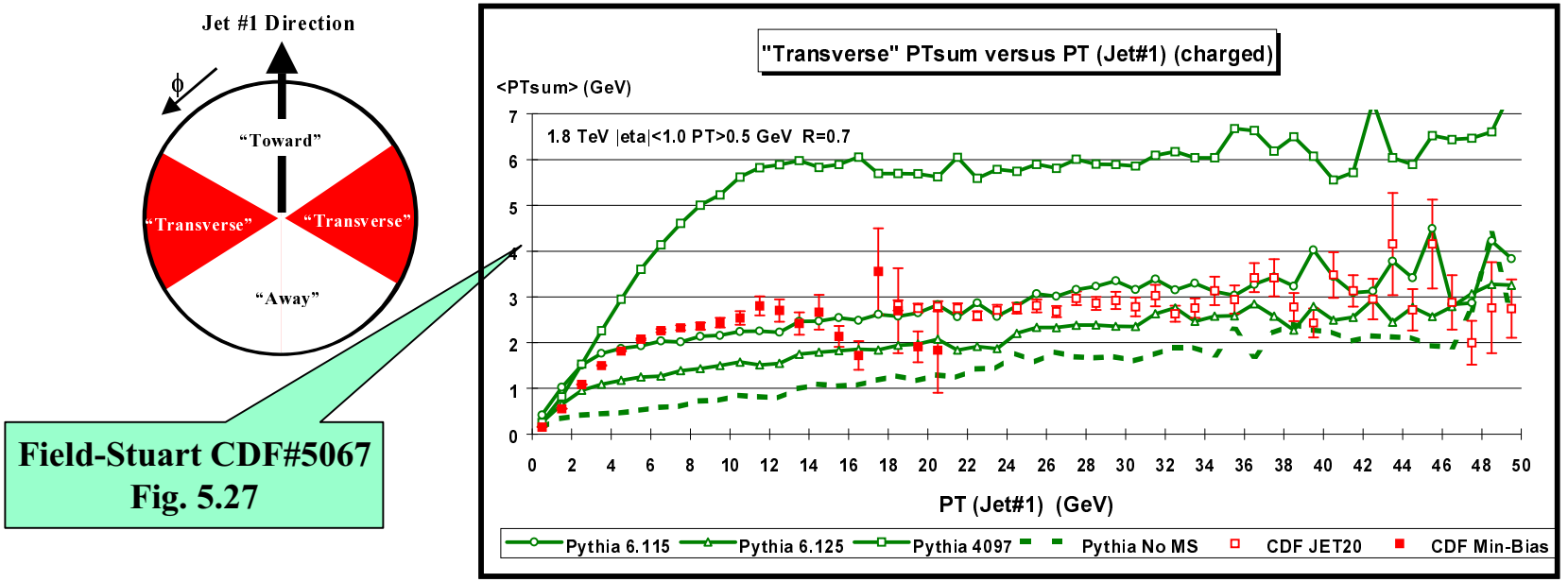

- Look at the charged PT flow in ϕ relative to the direction of jet#1 ($|\eta| < 1$ $P_T > 0.5$ GeV). Use the JET20 data to extend the range to $0.5 <$ PT(jet#1) < 50 GeV. Define "Transverse" $60^o < |\phi - \phi jet| < 120^o$.
- Plot shows "Transverse" <PTsum> in the vs PT(jet#1) compared to the QCD "hard" scattering predictions of four versions of Pythia (6.115, 6.125, no multiple interactions, and CDF note 4097).